SEEQUENT

GeoStudio Example File

Passive Cooling of Permafrost by Air Convection

To see the latest GeoStudio learning content, visit Seequent Learning Centre and search the catalogue for “GeoStudio”.

Introduction

The construction of sustainable road, railway, and runway embankments in cold climates hinges on countering the changes to the surface energy balance that cause permafrost degradation. Goering (2000) investigated air convection embankments constructed of unconventional and highly porous materials as a means of countering these changes and preserving permafrost. Unstable air density stratifications within the highly porous materials were found to lead to the development of convective cells during the cold winter months. The convective cells enhanced energy transfer out of the earthen structure, resulting in passive cooling, which promoted preservation of the underlying permafrost.

The objective of this example is to simulate an air convection embankment in a northern climate using AIR/W and TEMP/W.

Background

Goering and Kumar (1996) used a finite element program to numerically demonstrate the passive cooling capability of air convection embankments. Goering (1998) provided strong experimental evidence of the cooling effect of these embankments. Goering (2000) extended the initial numerical and experimental studies by focusing on the air pressure boundary condition for the side-slope of the embankment and considering: (a) an open boundary which allowed for infiltration of ambient air, and (b) a closed boundary which allowed for internal convection without atmospheric interaction. This latter boundary condition is generally representative of a high moisture content topsoil cover or snow cover during the winter months.

Numerical Simulation

Figure 1 presents the finite element domain used to represent the air convection embankment and underlying ice-rich silt subgrade. Although not part of the domain, an impervious asphalt concrete layer is assumed to cover the horizontal surface of the embankment. The symmetrical nature of the problem allows for simulation of half of the domain. The embankment is 6 m wide, 2.5 m height with 2:1 side-slopes. The mesh density is increased within the embankment as well as the upper portion of the subgrade but decreased along the outside edges of the lower portion of the subgrade.

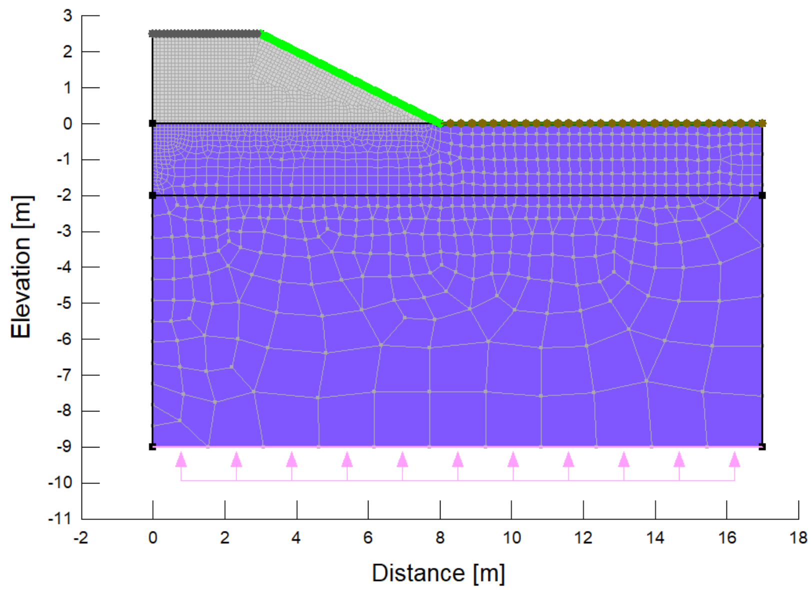

Figure 1. Finite element domain.

Figure 2 shows the analyses included in the project file. The first analysis establishes the initial conditions while the second and third analyses focus on heat conduction and both heat conduction and convection, respectively. In this latter case, both air and heat transfer processes are included and the free and forced convection options are toggle on (Figure 3). In so doing, the temperature is used to compute the air density and the air fluxes are used to compute the forced convection (or advection) heat transfer term. Although water is herein assumed immobile, water transfer (and associated free and forced convection) can be included by adding the appropriate physical processes.

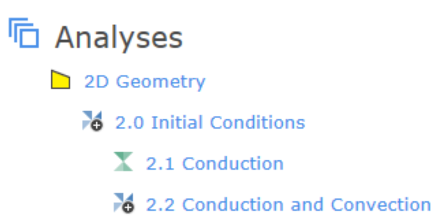

Figure 2. Project analyses tree.

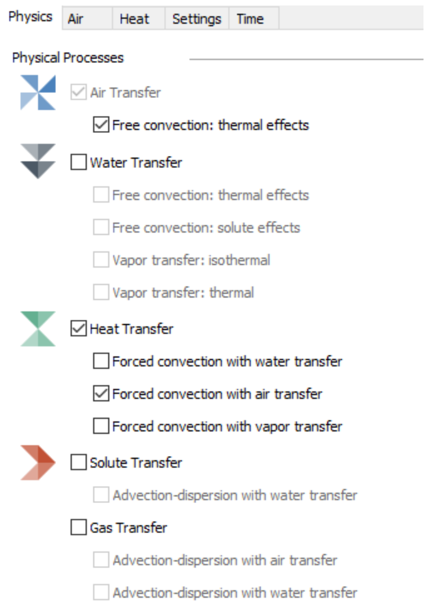

Figure 3. Settings on the physics tab.

The embankment and subgrade are defined using the simplified thermal and full thermal material models, respectively. The embankment material consists of a dry mixture of rock and gravel with volumetric heat capacity (frozen and unfrozen) and thermal conductivity (frozen and unfrozen) equal to 1020 kJ/m³/°C and 0.000346 kJ/sec/m/°C, respectively. The subgrade consists of an ice-rich silt with a volumetric water content of 0.649 m³/m³. The frozen and unfrozen volumetric heat capacity of the silt is equal to 1640 kJ/m³/°C and 2010 kJ/m³/°C, respectively. The thermal conductivity function is estimated using the sample silt material with a frozen and unfrozen thermal conductivity of 0.00215 kJ/sec/m/°C and 0.00200 kJ/sec/m/°C, respectively.

Given that the water is assumed immobile, the embankment and subgrade are represented by single-phase air material models. The air conductivity of the embankment material is computed as follows:

$$K = \frac{k\mu}{\gamma}$$ **Equation 1**

where k = 6.3 × 10^{-7} m² is the intrinsic permeability, μ = 1.72 × 10^{-5} kg/m/s is the dynamic viscosity of air at 0°C, and γ = 12.67 N/m³ is the unit weight of air at 0°C. It must be noted that the reference temperature (and resulting air conductivity) may differ from that used in Goering (2000). It should also be noted that extraordinarily high air conductivity may lead to extremely large air fluxes, which can create ill-conditioned global finite element matrices that result in premature termination of the solvers. Caution is therefore advised when dealing with uniformly graded coarse-grained materials. Although saturated, the air conductivity of the ice-rich silt subgrade is set equal to a non-zero value for numerical purposes. On this point, it should be noted that the arbitrary value should be large enough to prevent numerical ill-conditioning of the global finite element matrices.

Table 1. Annual harmonic temperature functions (Goering, 2000).

	N-factor Freezing	N-factor Thawing	Temperature function (°C)
Air	N/A	N/A	$-3.8 - 20.0 \cos[2\pi (t - 9) / 365]$
Asphalt Surface	0.9	1.9	$1.1 - 26.1 \cos[2\pi (t - 9) / 365]$
Side-Slope Surface	0.6	1.7	$2.7 - 20.9 \cos[2\pi (t - 9) / 365]$
Native Surface	0.5	0.5	$-1.9 - 10.0 \cos[2\pi (t - 9) / 365]$

The thermal boundary conditions consist of a combination of prescribed heat fluxes and temperatures. A geothermal heat flux of 6×10^{-5} kJ/s/m² is applied to the bottom surface of the domain while the vertical surfaces are considered adiabatic. The upper surfaces are subjected to annual harmonic temperature functions that are determined with surface specific N-factors and air temperature conditions corresponding to those observed in Fairbanks, Alaska. These functions are summarized in Table 1, where t is the time of the year. As expected, the functions have the same period and phase shift, but different mean and amplitude (Figure 4). It should be noted that the mean temperature at the surface of the native soil (- 1.9°C) promotes permafrost while the mean temperatures at the surfaces of the embankment (above 0°C) promote permafrost degradation. The outer surfaces of the domain are assumed impervious, and therefore modeled using zero flow boundary conditions. The transient analyses are initiated on the ninety-first day of the year when the surface temperatures are similar to the initial temperature. The analyses are solved over a twenty-five-year period to obtain the annual cycle that eventually develops in response to the applied boundary conditions and material properties. The results are saved on the first day of each month of the last years of the analysis.

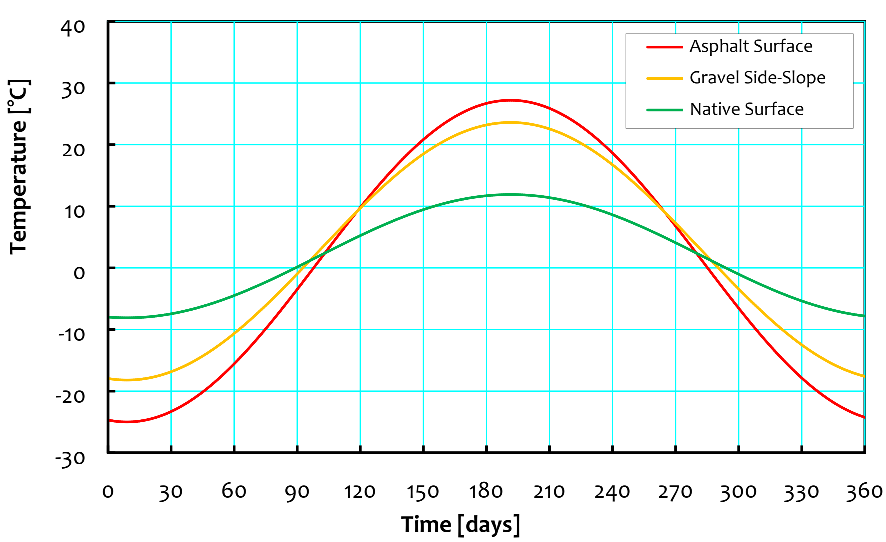

Figure 4. Harmonic temperature change with time.

Results and Discussion

Goering (2000) provides an insightful discussion on the physical processes operating to promote convective cooling. Only a brief summary of some of the highly relevant results are provided here. Figure 5 compares the simulated pore-air flux vectors (and convective cells) on February 1 of the twenty-fifth year of the analysis. Two large and dominating convective cells develop below the asphalt surface, circulating the pore air in clockwise and counter-clockwise directions. The mean magnitude of the pore-air flux (and more specifically, the mean of the nodal values of pore-air flux) is similar to that found in the reference study. Figure 6 shows the mean magnitude of the pore-air flux as a function of time. The mean pore-air flux increases from a minimum of 0.9 m/h, at the autumnal equinox, to a maximum of 11.8 m/h at the end of autumn. The mean pore-air flux generally decreases when the ambient air temperature increases and increases when the ambient air temperature decreases. The air convection embankment is therefore more effective at removing heat from the domain during wintertime than adding heat to the domain during summertime. As pointed out by Goering (2000), natural convection cells develop as the temperature difference between the upper and lower surfaces of the embankment exceeds a critical value. Natural convection is therefore more prevalent during the wintertime when the surface temperatures are low compared to the temperatures near the base of the embankment.

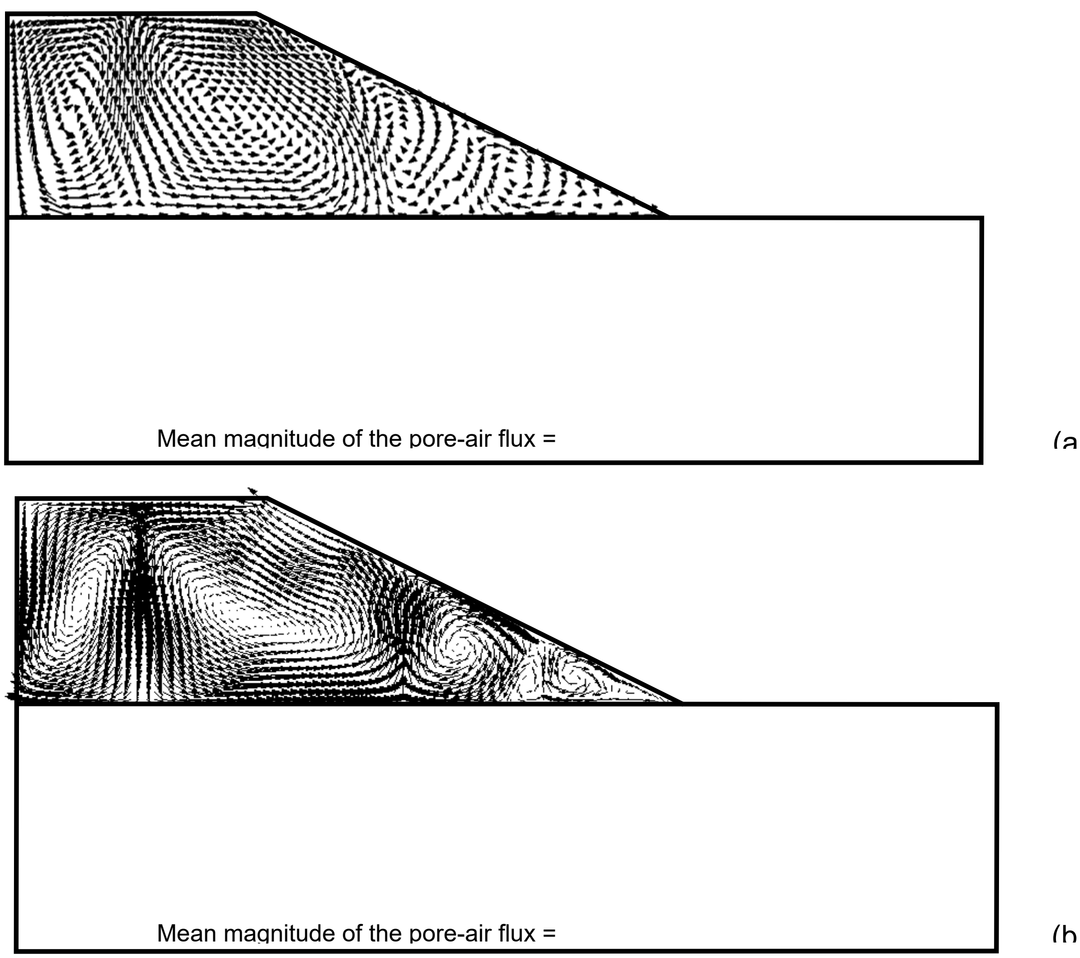

Figure 5. Air flux vectors on February 1. (a) Goering (2000). (b) AIR/W and TEMP/W.

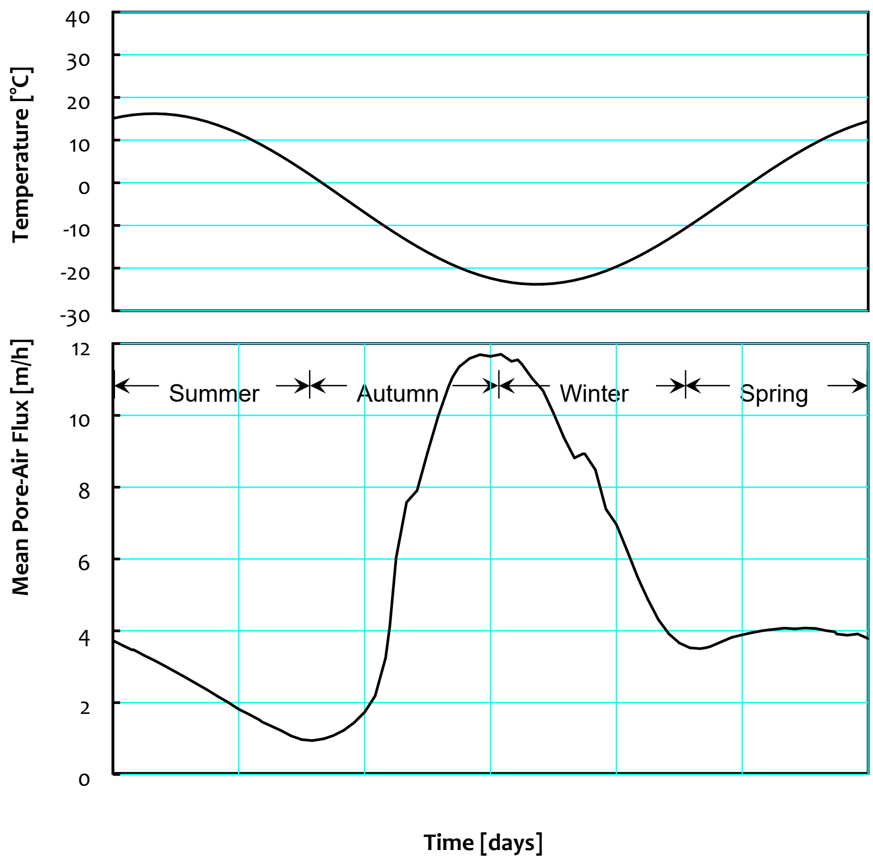

Figure 6. Annual variations of temperature and mean magnitude of pore-air flux.

Figure 7a shows the temperature contours that develop in the domain during wintertime. As expected, the results are in reasonable agreement with those found in the reference study. The discrepancies (which are most prevalent in the subgrade) are most likely ascribed to differences in material properties and the algorithms used to handle latent heat effects. The shape of the contours in the air convection embankment are highly influenced by the pore-air convection cells, which are formed due to unstable density stratification. As pointed by Goering (2000), the convection cells have a strong cooling effect on the subgrade soil below the embankment. This is evidenced by the position of the four-degree Celsius isotherm that lies almost as deep at the centerline as it does beneath the native surface, despite the presence of a rather thick (2.5 m) overburden at the centerline. Figure 7b shows the temperature contours during summertime. As expected, the contours remain relatively horizontal in the embankment in which conduction is the predominate heat transfer mechanism (very little to no convective mixing). As pointed out by Goering (2000), the zero isotherm doesn't progress as deeply in the subgrade soil beneath the embankment as it does beneath the native surface.

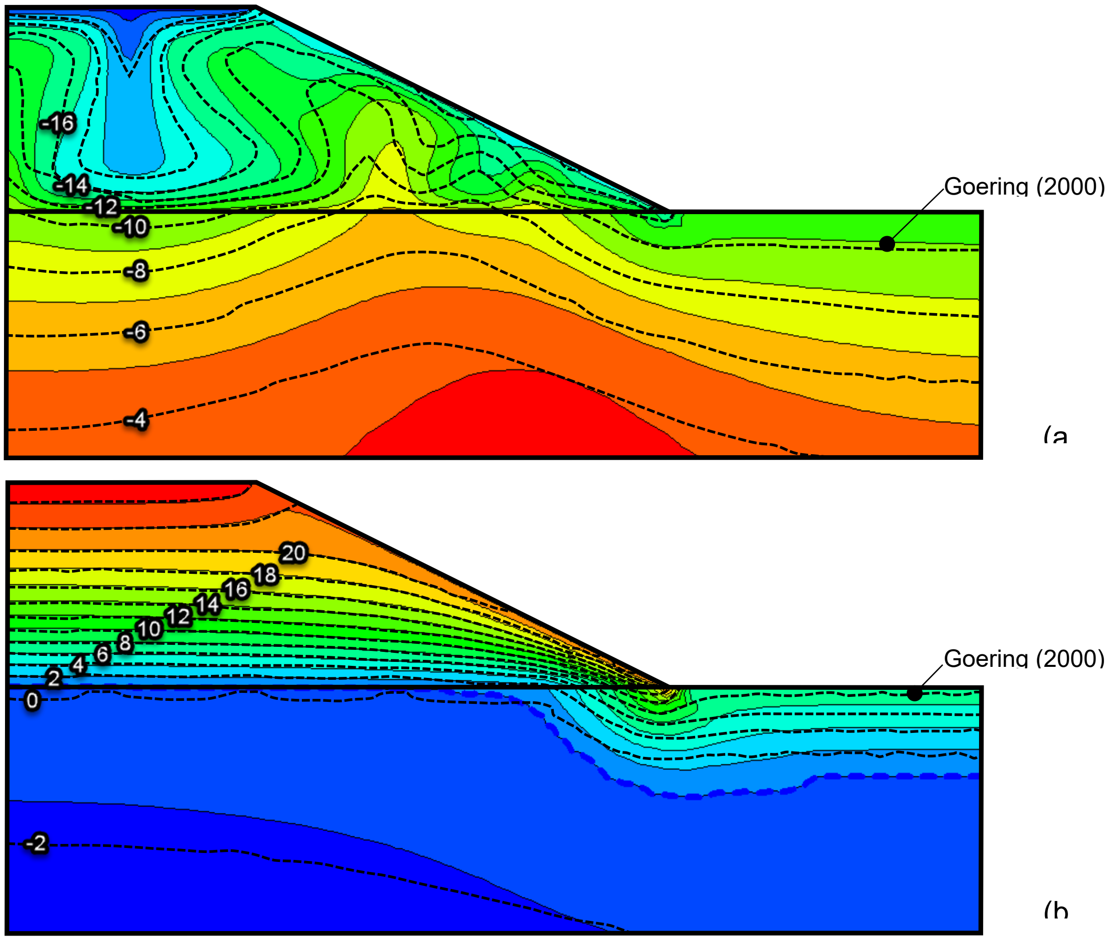

Figure 7. Temperature contours on (a) February 1. (b) August 1.

Goering (2000) provides field evidence of the passive cooling capability of an air convection embankment constructed in Fairbanks, Alaska. Although not covered with an impervious asphalt concrete layer, the geometry of the embankment corresponds to that used in the numerical analysis. Snow was removed from the ice-covered surface and plowed onto the side slope of the embankment to mimic actual road conditions. The side slope was also covered with a temporary impermeable plastic sheet during summertime. Figure 8 shows the measured temperature contours in the experimental embankment on February 1 and August 1. Despite considerable deviation from the numerical conditions, the contours provide unmistakable evidence of a strong downward plume beneath the driving surface during wintertime. The general agreement between experimental and numerical results helps elucidate the mechanisms at work in air convection embankments. The experimental and numerical results also indicate that air convection embankments can be used as means of countering the changes to the surface energy balance that cause permafrost degradation.

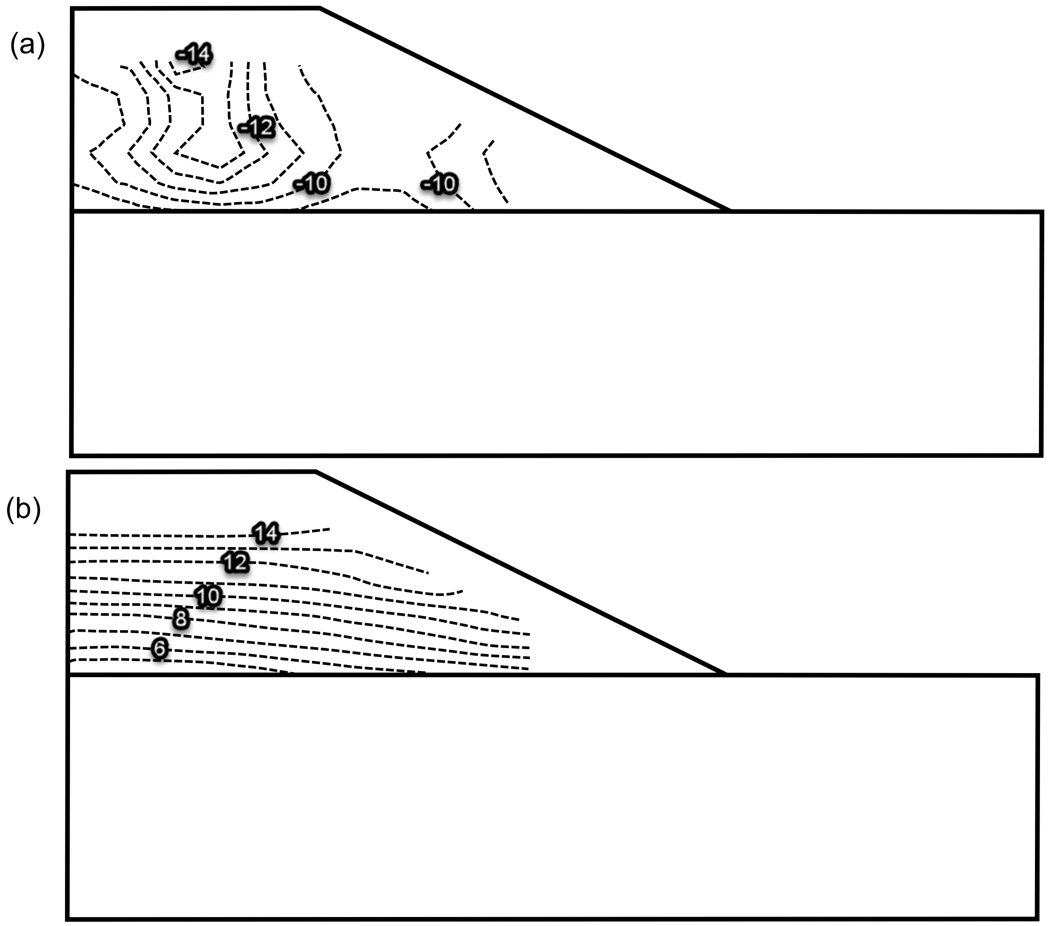

Figure 8. Measured temperature contours (Goering, 2000). (a) February 1. (b) August 1.

Summary and Conclusions

AIR/W and TEMP/W were used to simulate an air convection embankment in a northern climate. Unstable air density stratifications in the embankment material were found to lead to convective cells during wintertime. The convective cells resulted in passive cooling that prevented thawing of the permafrost, thus eliminating thaw settlement. A note of caution, however, the convective cells that are beneficial in northern climates can enhance seasonal freezing of the subgrade and exacerbate problems with frost heave in temperate climates.

References

Goering, D.J. and Kumar, P. 1996. Winter-time convection in open-graded embankments. Cold Regions Science and Technology, 24, 57-74.

Goering, D.J. 1998. Experimental investigation of air convection embankments for permafrost-resistant roadway design. Proceedings of the 7th International Conference on Permafrost, Yellowknife, NWT, 319-326.

Goering, D.J. 2000. Passive cooling of permafrost foundation soils using porous embankment structures. Proceedings of the Heat Transfer Division, ASME International Mechanical Engineering Congress and Exposition, Orlando, Florida, 103-111.